

---

# Observations and Modeling of Turbulence in the Solar Wind

Melvyn L. Goldstein

NASA Goddard Space Flight Center, USA

E-mail: melvyn.l.goldstein@nasa.gov

**Summary.** Alfvénic fluctuations are a ubiquitous component of the solar wind. Evidence from many spacecrafts indicate that the fluctuations are convected out of the solar corona with relatively flat power spectra and constitute a source of free energy for a turbulent cascade of magnetic and kinetic energy to high wave numbers. Observations and simulations support the conclusion that the cascade evolves most rapidly in the vicinity of velocity shears and current sheets. Numerical solutions of the magnetohydrodynamic equations have elucidated the role of expansion on the evolution of the turbulence. Such studies are clarifying not only how a turbulent cascade develops, but also the nature of the symmetries of the turbulence.

**Key words:** Magnetohydrodynamics-solar wind: Turbulence-simulations

## 1 Observed Properties of the Solar Wind

The solar wind is the continuous outflow of ionized gas from the solar corona [1]. It is composed primarily of supersonic protons. Alpha particles comprise a few percent of the total and there are traces of heavier ions. The ion flow is generally about Mach 10. In contrast, the electrons are subsonic with a Mach number of  $\approx 0.2$ . Although the temperature of the corona is typically 1 – 2 MK, the temperature of electron and protons near Earth orbit is only about a tenth of that. The flow becomes supersonic within a few solar radii. Because the solar wind plasma is highly conductive, the “frozen-in” coronal magnetic field is pulled into the interplanetary medium by the flow and solar rotation winds it into an “Archimedean” spiral pattern [2]. The wind rapidly attains a nearly constant terminal speed after which its density decreases as the square of the radial distance from the sun.

### Solar wind flow patterns

Solar wind flow patterns vary with solar cycle. The most well-organized patterns occur during times of minimum solar activity when there are regions of

steady fast wind that originate from regions of open magnetic field lines where the corona is cooler than in surrounding loops. These regions appear darker in EUV and X-ray wavelengths and are referred to as *coronal holes*. Fast solar wind has speeds exceeding 600 km/s and can reach  $\approx 800$  km/s. Slow solar wind, which is rather unsteady, has speeds less than about 500 km/s and originates near closed loops and coronal streamers. This region is also associated with coronal mass ejections (CMEs) that generate highly transient flows that include large-scale magnetic clouds.

## 1.1 Alfvén Waves

Soon after the discovery of the solar wind it was realized [4, 5, 6, 11, 43] that the fluctuations in the magnetic field and velocity were often so highly correlated that they appeared as nearly perfect Alfvén waves [3]. This phenomenon was most pronounced in fast solar wind, especially in the trailing edges of the fast streams. However, highly “Alfvénic” flows have been observed in slow wind as well.

If one normalizes the fluctuating magnetic field,  $\mathbf{b}$ , by dividing by  $\sqrt{\mu_0 \rho}$  (where  $\rho$  is the mass density), Alfvén waves are defined by  $\mathbf{v} \equiv \pm \mathbf{b}$ , where  $\mathbf{v}$  is the fluctuating component of the velocity. The  $\pm$  sign represents wave propagation antiparallel (+) and parallel (−) to the ambient magnetic field. It is often convenient to use new variables, referred to as Elsässer variables that are defined by  $\mathbf{z}^\pm = \mathbf{v} \pm \mathbf{b}$ . The predominance of outward propagation suggests that the Alfvénic fluctuations are generated below the height where the flow becomes super-Alfvénic. Thus, only outward propagating fluctuations are convected into the heliosphere.

An example of an Alfvénic interval is shown in Figure 1 from data taken by Ulysses during a polar pass. The data are displayed as component fluctuations in Sun-Earth-Ecliptic coordinates (radial, normal, tangential, i.e., RTN) of the magnetic field (thin lines) and velocity vector (thick lines). The high correlations, also referred to as high *Alfvénicity*, are obvious, and the positive sense of correlation for sunward-pointing magnetic field implies that the fluctuations are propagating outward.

The very high Alfvénicity of solar wind fluctuations might lead one to wonder whether or not the medium is actively evolving because *pure* Alfvén waves are an exact solution of the incompressible, ideal, equations of magnetohydrodynamics. However, the solar wind also exhibits the contrasting quality, first noted by [12], viz., that the power spectra of the magnetic (and velocity) fields resemble that of fully developed fluid turbulence [24] in that the spectral index of the power spectra is  $\approx -5/3$ . Analyses of Helios data show, however, that while the power spectra of fluctuations observed in slow wind and in fast wind at 1 AU (and beyond) typically have an “inertial range” spectrum with a slope of  $-5/3$ , at 0.3 AU in fast wind, only a very limited inertial range exists and the spectrum is dominated by an extended energy-containing range with an spectral index of  $-1$ .

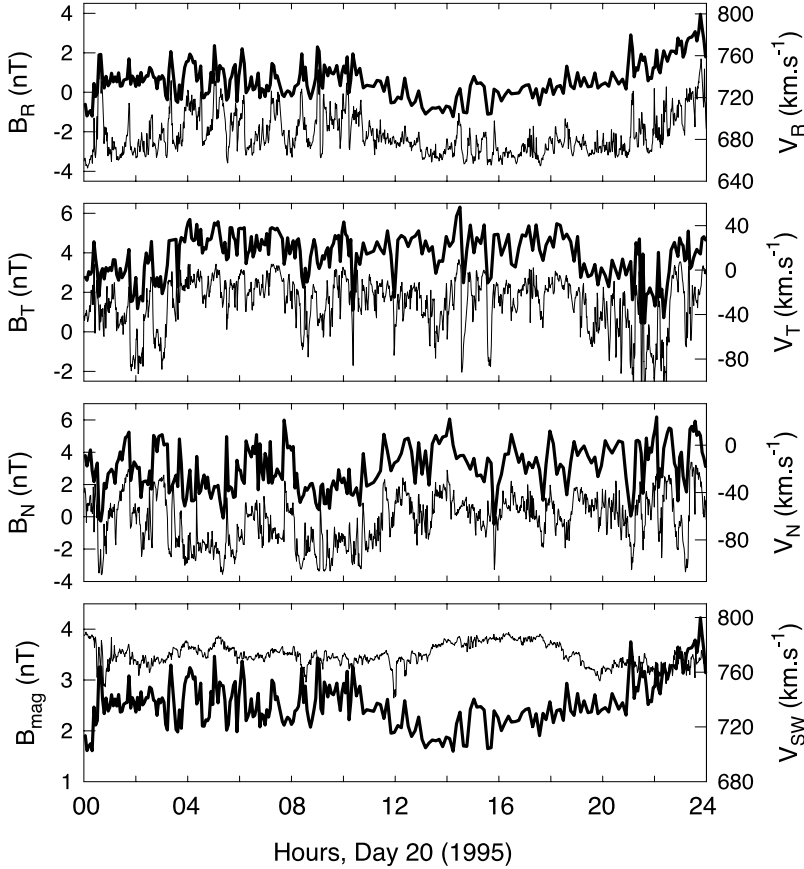


**Fig. 1.** RTN components and magnitude of the solar wind magnetic field (thin line, left hand scale) and those of the velocity of the solar wind (thick line, right hand scale) measured by Ulysses in the fast solar wind.

### Relationship of Solar Wind Turbulence to Fluid Turbulence

In Figure 2 we show the classic example of fully developed fluid turbulence [20], and, for comparison, in Figure 3, an example computed from Voyager magnetometer data obtained near 1 AU [26]. Figure 4 shows the difference between fast and slow wind at 0.3 AU from [42]. The Helios data have been plotted using Elsässer variables,  $z^\pm$ .

As is clear from these spectra, when turbulence has had the opportunity to develop an inertial range, the slope is essentially  $-5/3$ , the Kolmogorov value for fully developed, incompressible Navier-Stokes fluid turbulence. The remarkable result is still not fully understood, because the solar wind is neither a Navier-Stokes fluid nor is it incompressible.

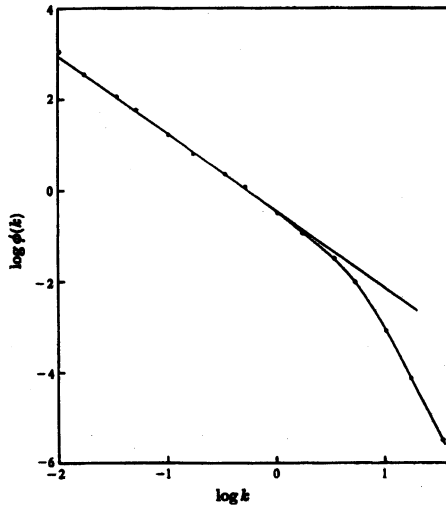


**Fig. 2.** A plot of the one-dimensional spectrum of tidal channel data collected on March 10, 1959. The straight line has a slope of  $-5/3$ . From [20].

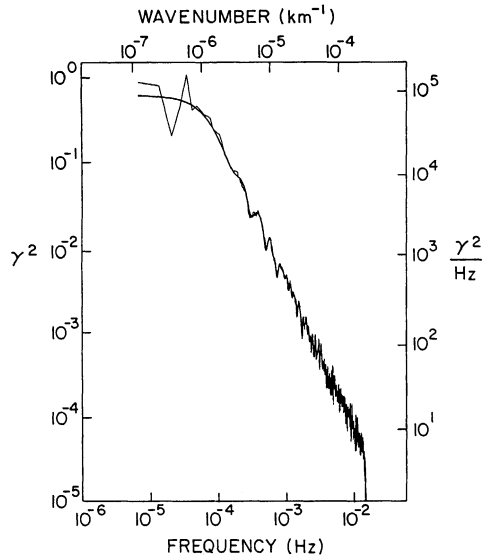


**Fig. 3.** The magnetic energy spectrum of data collected at 1 AU in units of  $\text{nT}^2$ . The abscissa is given in both frequency and wave number. Spectra constructed using the Blackman-Tukey algorithm [8] and the fast Fourier transform technique are shown. To an excellent approximation, the slope of the power spectrum is  $-5/3$ .

[12] noted the strong association of a well-defined  $-5/3$  inertial range with (slow) flows that were found in the vicinity of the heliospheric current sheet where velocity gradients tend to be large and where the magnetic field changes sign as one crosses the current sheet. [12] argued that turbulence in the solar wind was driven by the energy in velocity shears. [36], in an extensive analysis of Helios data, confirmed this conjecture.

## Properties of Solar Wind Turbulence

The variation in the degree of Alfvénicity of the magnetic and velocity fluctuation with both distance and with latitude have been an intense area of study. In a series of papers, [36, 38] examined the evolution of the solar wind with distance using data from both Helios and Voyager. That analysis showed clearly that in the outer heliosphere the Alfvénicity tended to decrease—higher wave numbers retained their Alfvénic nature to larger heliospheric distances. (There are exceptions to this as discussed in [38]).

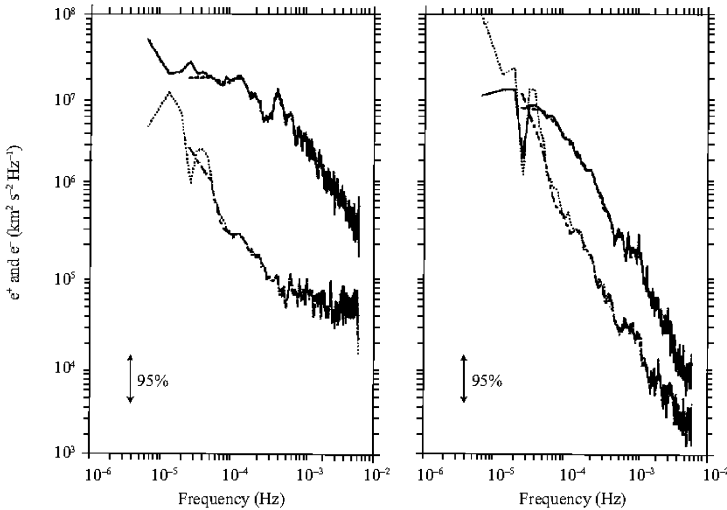


**Fig. 4.** Power spectra of the Elsässer variables for fast wind (left panel) and slow wind (right panel) from data obtained by Helios at 0.3 AU. Adapted from [42].

Data from Ulysses gives another view of how Alfvénic fluctuations evolve in the heliosphere. Evolution should be quite slow at the high heliospheric latitudes probed by Ulysses because there velocity gradients are small; and indeed, the fluctuations remain Alfvénic even near 4 AU at those high latitudes, as is illustrated in Figure 5 [21, 23].

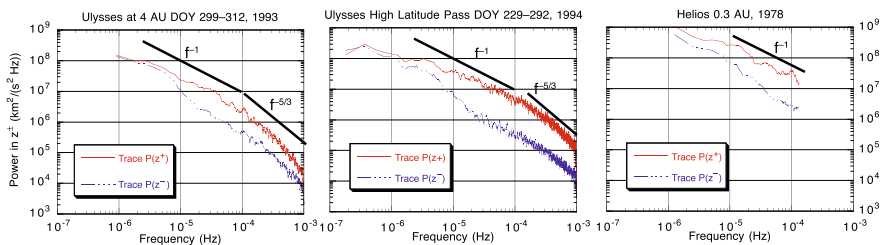


**Fig. 5.** The spectrum from Ulysses at 4 AU (left) are not very Alfvénic, while the spectrum from the high latitude pass (center) shows little evolution with latitude. The Helios spectrum (right) also suggests that the source spectrum of solar wind fluctuations is both highly Alfvénic and has a spectral slope of  $-1$  (cf. Figure 4, above). Adapted from [17].

## 1.2 Radial and Temporal Evolution of Solar Wind Turbulence

Another measure of Alfvénicity is the cross helicity, defined by

$$H_c = \frac{1}{2} \int dx^3 \mathbf{v} \cdot \mathbf{b}.$$

A useful related quantity is the normalized cross helicity, defined by  $\sigma_c \equiv 2H_c^r(k)/E^r(k)$ , where  $E^r(k)$  is the reduced spectral energy (magnetic plus kinetic). These quantities are reduced in the sense that, due to the super-Alfvénic nature of the solar wind flow, the one-dimensional power spectra are equivalent to three-dimensional spectra that have been integrated over perpendicular wave numbers [26].

A clear indication that velocity shear is the primary driver of solar wind turbulence and the cause of the reduction with heliocentric distance of cross helicity is shown in Figure 6. In the figure, the normalized cross helicity,  $\sigma_c$ , which is generally close to unity in fast wind, fluctuates around zero where  $B_R$  changes sign and where the velocity gradients are large. This situation has been simulated using both two-dimensional incompressible and compressible codes in Cartesian (periodic) geometry as well as in three dimensions in spherical geometry [18]. The two-dimensional results are shown in Figure 7. The top panel shows results at  $T = 4$  eddy-turnover times from an incompressible MHD simulation, where  $\omega \equiv \nabla \times \mathbf{v}$  is the vorticity. The bottom panel shows similar results at  $T = 2$  eddy-turn-over times from a solution of the compressible equations.

## 1.3 The Symmetry Properties of the Magnetic Fluctuations

The magnetic and velocity field fluctuations in the solar wind are intrinsically three-dimensional. However, as mentioned above, the supersonic/super-Alfvénic nature of the flow makes it difficult with only single point measurements to determine more than the reduced, one-dimensional, properties of the

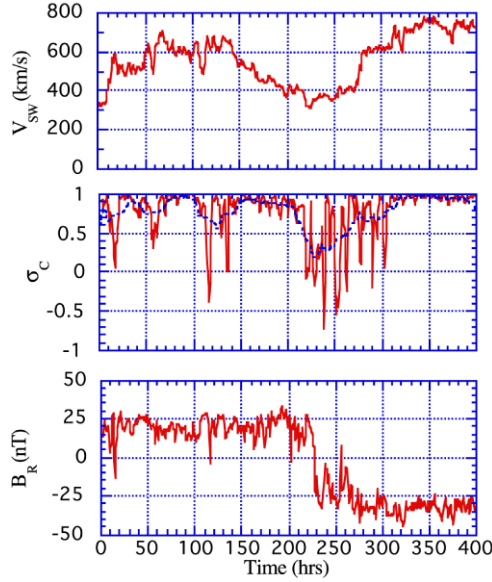


**Fig. 6.** A current sheet crossing observed by Helios 2 near 0.3 AU (days 93 – 110 of 1976). The data are hour averages. The blue curve of  $\sigma_c$  is a 25-hour running mean. The minimum values of  $\sigma_c$  are found in the low speed region where  $B_R$  changes sign and where the velocity gradients are large. Adapted from [34] and [37]

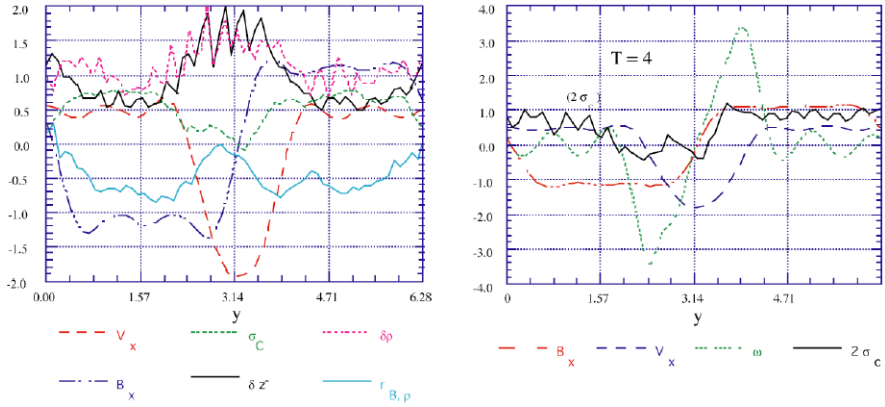


**Fig. 7.** Left: Results at  $T = 2$  eddy-turn-over times from a solution of the compressible equations. The panel includes density fluctuations,  $\rho$ ,  $\delta z_-$ , and the correlation between density and magnetic field magnitude,  $r_B$  ( $\delta \rho$  and  $\delta z_-$  are normalized to twice their maximum values of 0.042 and 0.075, respectively). Right: The solution at  $T = 4$  eddy-turnover times from an incompressible simulation ( $\omega$  is the vorticity). From [35]

fluctuations. It is possible, however, even with a single spacecraft (and some additional assumptions) to explore at least two-dimensional symmetries. [40] analyzed the relatively few intervals during which the background magnetic field  $\mathbf{B}$  was either parallel or transverse to the solar wind velocity. Because of a paucity of examples they could not reach any definitive conclusions, but suggested that the magnetic fluctuations could not be isotropic, although for periods when  $\mathbf{B}$  was perpendicular to the solar wind velocity, the isotropic model was a reasonable approximation and parallel propagating Alfvén waves offered a poor approximation that was only approximately valid during the radial  $\mathbf{B}$  flow intervals. They suggested that a combination of magnetosonic and Alfvén waves with approximately one quarter as much power in magnetosonic waves as in Alfvén waves fit both data intervals.

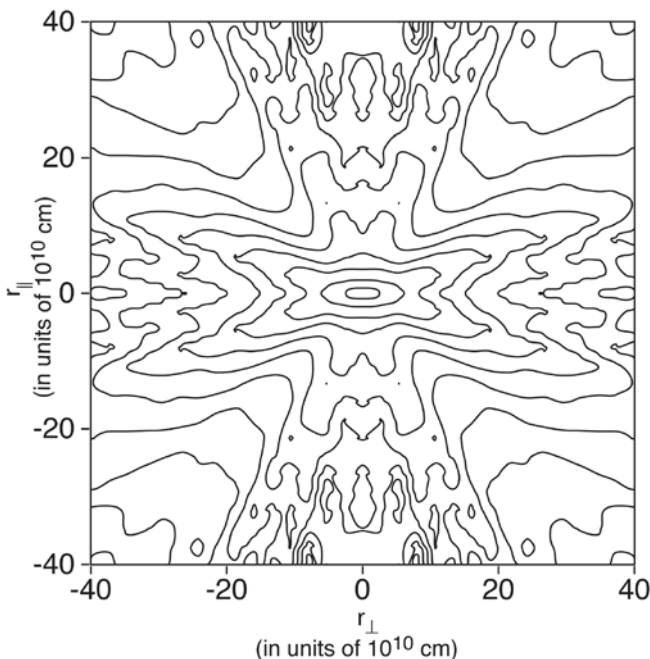


**Fig. 8.** Contour plot of the two-dimensional correlation function of solar wind fluctuations as a function of distance parallel and perpendicular to the mean magnetic field. The four quadrant plot was produced by reflecting the data across the axes from the first quadrant (from [29]).

The first comprehensive effort to deduce at least the two-dimensional structure of the magnetic fluctuations was carried out using approximately 16 months of nearly continuous data from ISEE 3 by [29]. The results suggested that the solar wind fluctuations were made of two components: parallel prop-



agating planar (slab) Alfvén waves and fluctuations with wave vectors nearly transverse to the mean magnetic field. The analysis was done on stationary data intervals [27, 28, 31, 33] and assumed that all the data intervals (463 15-min averages) were members of the same statistical ensemble. The two-dimensional correlation function from that analysis is shown in Figure 8. More recently, [13] has carried out a similar analysis, but the intervals were sorted by whether the flows were fast or slow. They concluded that the fast and slow wind belonged to separate ensembles and that fast wind was more dominated by slab-like fluctuations and slow wind contained more quasi-two-dimensional fluctuations.

[7] suggested that typically 80% of the magnetic fluctuation energy resided in the quasi-two-dimensional component and only 20% was in the “slab” component. Subsequently, [41], using Ulysses data, showed that between 1991 and 1995, a more typical value was 50%. There was no obvious way to tell, however, whether the “quasi-2D component” reflected a nearly-incompressible population of fluctuations or merely one that contained nearly perpendicular wavevectors.

[39] used a three-dimensional spherical simulation to demonstrate that small velocity shears would produce rapid “phase mixing” of planar Alfvén waves. [19] later generalized the results of [15, 16] to three dimensions, showing that small velocity shears superposed on an initial wave packet of planar Alfvén waves could evolve with distance to produce two-dimensional correlation functions reminiscent of the ISEE-3 analysis.

Consequently, it appears that the 50 – 80% of the fluctuation energy that is quasi-two-dimensional, does not reflect a nearly-incompressible component of the turbulence that arose in the corona, but rather indicates either local generation or phase mixing. Ascertaining the nature of these fluctuations is important because the distribution of power between parallel and perpendicular wave numbers determines the spatial diffusion of solar and galactic energetic particles since only power in  $k_{\parallel}$  resonantly scatters energetic charged particles.

## 2 Simulating Solar Wind Turbulence

The evolution of turbulence in a spherically expanding magnetofluid such as the solar wind requires solving the MHD equations using a finite difference algorithm. One approach has been to use fourth-order flux corrected transport (FCT) [9, 14, 44, 18], although other approaches and algorithms have been used. In the approach used by [18], the magnetic field is determined using Faraday’s law, which ensures that  $\nabla \cdot \mathbf{B} = 0$  is preserved to within numerical round-off errors. The dependent variables are density,  $\rho$ , momentum  $\rho \mathbf{v}$ , total energy (internal  $(\rho e) +$  kinetic  $(\rho v^2/2) +$  magnetic  $(B^2/2\mu_0)$ ), and the magnetic field  $\mathbf{B}$ . The equation of state is that of an ideal gas ( $p = \rho RT$ ), where  $R$  is the gas constant and  $T$  is temperature.

The turbulence solutions are initiated with supersonic/super-Alfvénic time-dependent inflow boundary conditions that are imposed at some radial distance above the critical point, typically taken to be between  $r = 0.2 - 0.5$  AU. The solutions include a tilted rotating current sheet, incoming Alfvénic or two-dimensional modes with finite transverse correlation lengths, microstreams, and pressure-balanced structures.

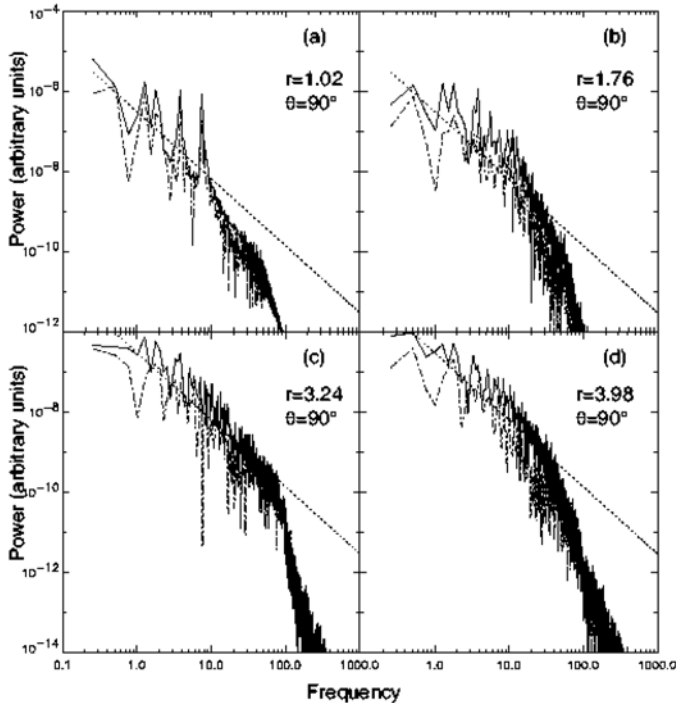


**Fig. 9.** Power spectra deduced from the time series of the magnetic field components and  $|B|$  (dashed line) along a radius in slow speed flow at  $\theta = 90^\circ$  and four radii ranging from  $r = 1.02 - 3.98$  AU. Also shown on each plot is a line with slope of  $-5/3$ . From [18].

## 2.1 Simulations of a Turbulent Cascade

Using algorithms that are sufficiently dissipationless, one can study the development of a cascade of magnetic energy from the input energy-containing scales toward the dissipation range. Eventually, the residual numerical dissipation does steepen the spectrum and damp fluctuations. In Figure 9, a series of

power spectra are plotted that were computed from a time series of magnetic field values taken at four sites in the simulation domain. Simulation output is for “slow” flow near  $\theta = 90^\circ$  at four radial points ranging from 1.02–3.98 AU. This region near the current sheet, stirred as it is by strong velocity gradients and weak magnetic fields, is where the most rapid evolution takes place. The turbulent mixing generates about a decade of inertial range. The straight line on the plots has a slope of  $-5/3$ .

### 3 Summary

This brief review has omitted many topics in solar wind turbulence studies. Many questions remain unanswered. For example, we do not know if the corona is turbulent. Indications from Helios observations suggest that it is not, but rather that fluctuations are continuously pumping the medium via a log-normal process [30] that results in a  $k^{-1}$  power spectrum at the transition to the solar wind. A curious aspect of the Alfvénic turbulence in the solar wind is that their minimum variance direction tends to lie along the direction of the local magnetic field (see, for example, [22]). This simple observation has yet to be satisfactorily explained and simulations have been unsuccessful in replicating the observations. Recently [32], magnetic field data obtained by the four Cluster spacecraft when their separation reached 10,000 km has been used to compute wavenumber spectra parallel and perpendicular to the local magnetic field. Those preliminary results suggest that, indeed, quasi-two-dimensional fluctuations predominate over slab Alfvénic fluctuations. For a review of the theory of the solar wind, see [25]. An extensive review of solar wind observations, including topics such as intermittency that have not been mentioned here, can be found in the Living Reviews article by [10].

### References

1. Parker, E.N.: ApJ vol. 128, p 664 (1958)
2. Parker, E.: Interplanetary Dynamical Processes. Wiley, New York (1963)
3. Alfvén, H.: Cosmical Electrodynamics. Clarendon, Oxford (1950)
4. Barnes, A.: Rev. Geophys. vol. 17, p 596 (1979a)
5. Barnes, A.: Hydromagnetic waves and turbulence in the solar wind. In: Parker, E.N., Kennel, C.F., Lanzerotti, L.J. (eds.) Solar System Plasma Physics, vol. 1 p 249 North-Holland, Amsterdam (1979b)
6. Belcher, J.W., Davis, L.: J. Geophys. Res. vol. 76, p 3534 (1971)
7. Bieber, J.W., Wanner, W., Matthaeus, W.H.: J. Geophys. Res. vol. 101(A2), p 2511 (1996)
8. Blackman, R., Tukey, J.: Measurement of Power Spectra. Dover, New York (1958)
9. Boris, J.P., Book, D.L.: J. Comput. Phys. vol. 11, p 38 (1973)

10. Bruno, R., Carbone, V.: *Living Reviews in Solar Physics* **2**(4) (2005).  
<http://www.livingreviews.org/lrsp-2005-4>
11. Coleman, P.J.: *Phys. Rev. Lett.* vol. 17, p 207 (1966)
12. Coleman, P.J.: *ApJ* vol. 153, p 371 (1968)
13. Dasso, S., Milano, L.J., Matthaeus, W.H., Smith, C.W.: *ApJ* vol. 635(2), p L181 (2005)
14. DeVore, C.R.: *J. Comput. Phys.* vol. 92, p 142 (1991)
15. Ghosh, S., Matthaeus, W.H., Roberts, D.A., Goldstein, M.L.: *J. Geophys. Res.* vol. 103(A10), p 23691 (1998a)
16. Ghosh, S., Matthaeus, W.H., Roberts, D.A., Goldstein, M.L.: *J. Geophys. Res.* vol. 103(A10), p 23705 (1998b)
17. Goldstein, B.E., Smith, E.J., Balogh, A., Horbury, T.S., Goldstein, M.L., Roberts, D.A.: *Geophys. Res. Lett.* vol. 22(23), p 3393 (1995)
18. Goldstein, M.L., Roberts, D.A., Deane, A.E., Ghosh, S., Wong, H.K.: *J. Geophys. Res.* vol. 104(A7), p 14437 (1999)
19. Goldstein, M.L., Roberts, D., Deane, A.: In: Velli, M., Bruno, R., Malara, F. (eds.) *Solar Wind 10. AIP Conf. Proceedings*, vol. 679, 405. Amer. Inst. Phys. (2003)
20. Grant, H.L., Stewart, R.W., Moilliet, A.: *J. Fluid Mech.* vol. 12, p 241 (1962)
21. Horbury, T.S., Balogh, A.: *J. Geophys. Res. (Space)* vol. 106(A8), p 15929 (2001)
22. Horbury, T.S., Balogh, A., Forsyth, R.J., Smith, E.J.: *Geophysical Research Letters* vol. 22, p 3405 (1995)
23. Horbury, T.S., Balogh, A., Forsyth, R.J., Smith, E.J.: *Astron. Astrophys.* vol. 316(2), p 333 (1996)
24. Kolmogorov, A.N.: *Dokl. Akad. Nauk SSSR* vol. 30, p 299 (1941)
25. Marsch, E., Axford, W.I., McKenzie, J.M.: In: Dwivedi, B.N. (ed.) *Dynamic Sun*, 374. Cambridge Univ. P. (2003)
26. Matthaeus, W.H., Goldstein, M.L.: *J. Geophys. Res.* vol. 87, p 6011 (1982)
27. Matthaeus, W.H., Goldstein, M.L.: *J. Geophys. Res.* vol. 87, p 10347 (1982)
28. Matthaeus, W.H., Goldstein, M.L., King, J.H.: *J. Geophys. Res.* vol. 91, p 59 (1986)
29. Matthaeus, W.H., Goldstein, M.L., Roberts, D.A.: *J. Geophys. Res.* vol. 95, p 20673 (1990)
30. Matthaeus, W., Goldstein, M.L.: *Phys. Rev. Lett.* vol. 57, p 495 (1986)
31. Monin, A.S., Yaglom, A.M.: *Statistical Fluid Mechanics: Mechanics of Turbulence*. vol. 2. MIT Press, Cambridge, Mass. (1975)
32. Narita, Y., Glassmeier, K.H., Goldstein, M.L., Treumann, R.A.: In: Shaikh, D., Zank, G.P. (eds.) *Turbulence and Nonlinear Processes in Astrophysical Plasmas; 6th Annual International Astrophysics Conference, APS*, p 215. American Physical Society, Oahu, Hawaii (USA) (2007)
33. Panchev, S.: *Random Functions and Turbulence*. Pergamon, New York (1971)
34. Roberts, D.A., Ghosh, S., Goldstein, M.L., Matthaeus, W.H.: *Phys. Rev. Lett.* vol. 67, p 3741 (1991)
35. Roberts, D.A., Goldstein, M.L.: *Turbulence and waves in the solar wind*. In: Shea, M.A. (ed.) *U.S. National Report to International Union of Geodesy and Geophysics*, p 932. Amer. Geophys. Union, Washington DC (1991)
36. Roberts, D.A., Goldstein, M.L., Klein, L.W., Matthaeus, W.H.: *J. Geophys. Res.* vol. 92, p 12023 (1987a)

37. Roberts, D.A., Goldstein, M.L., Matthaeus, W.H., Ghosh, S.: J. Geophys. Res. vol. 97, p 17115 (1992)
38. Roberts, D.A., Klein, L.W., Goldstein, M.L., Matthaeus, W.H.: J. Geophys. Res. vol. 92, p 11021 (1987b)
39. Ruderman, M.S., Goldstein, M.L., Roberts, D.A., Deane, A., Ofman, L.: J. Geophys. Res. vol. 104(A8), p 17057 (1999)
40. Sari, J.W., Valley, G.C.: J. Geophys. Res. vol. 81, p 5489 (1976)
41. Smith, C.W.: In: Velli, M., Bruno, R., Malara, F. (eds.) Solar Wind 10. AIP Conf. Proceedings, vol. 679, 413. Amer. Inst. Phys. (2003)
42. Tu, C.Y., Marsch, E., Thieme, K.M.: J. Geophys. Res. vol. 94(A9), p 11739 (1989)
43. Unti, T.W., Neugebauer, M.: Phys. Fluids vol. 11, p 563 (1968)
44. Zalesak, S.T.: J. Comp. Phys. vol. 31, p 335 (1979)

Turbulence, Dynamos, Accretion Disks, Pulsars and  
Collective Plasma Processes

First Kodai-Trieste Workshop on Plasma Astrophysics  
held at the Kodaikanal Observatory, India, August 27 -  
September 7, 2007

Hasan, S.; Gangadhara, R.; Krishan, V. (Eds.)

2008, XIII, 342 p., Hardcover

ISBN: 978-1-4020-8867-4